European Review for Medical and Pharmacological Sciences 2018; 22: 8866-8876

Hypoxia is involved in hypoxic pulmonary hypertension through inhibiting the activation of FGF2 by miR-203

L.-N. WANG, W.-C. YU, C.-H. DU, L. TONG, Z.-Z. CHENG

Department of Respiratory Medicine, The Affiliated Hospital of Qingdao University, Qingdao, China

Abstract. – OBJECTIVE: The aim of this study was to investigate whether hypoxia *in vivo* can induce hypoxic pulmonary hypertension by inhibiting the activation of FGF2 by miR-203.

MATERIALS AND METHODS: We established a rat model of hypoxic pulmonary hypertension (HPH), and measured the right ventricular systolic pressure (RVSP) and right ventricular hypertrophy (right ventricular hypertrophy index). The ventricular hypertrophy index (RVHI) was calculated and HE staining of the lung tissue of HPH rats was performed. We extracted pulmonary arterial smooth muscle cells (PASMCs) from rats and identified them by immunofluorescence assay. The expression of miR-203 in hypoxic PASMCs was detected by quantitative Real time-polymerase chain reaction (qRT-PCR). The proliferation and migration of PASMCs were detected by EDU (5-Ethynyl-2'-deoxyuridine), cell counting kit-8 (CCK-8) and scratch assay, respectively. Dual Luciferase reporting assay and Western blot were used to detect the binding of miR-203 and FGF2.

RESULTS: The results of qRT-PCR showed that miR-203 expression in rat PASMCs was significantly lower than that in normoxia control group at 24 h and 48 h after hypoxic treatment. EDU, CCK8 and scratch test results showed that proliferation and migration ability of PASMCs were weakened after overexpression of miR-203, and vice versa. Dual Luciferase reporter gene assays and Western blot experiments showed that miR-203 could target and combine with FGF2 to inhibit its expression. *In vivo* experiments showed that low expression of FGF2 could lead to decreased RVSP and RVHI, decreased FGF2 protein levels, and decreased WT% and (PM+FM)% in hypoxia-treated rats.

CONCLUSIONS: Hypoxia *in vivo* is involved in the development of HPH by inhibiting the activation of FGF2 by miR-203. Meanwhile, specific inhibition of FGF2 can reduce hypoxia-induced pulmonary hypertension and improve pulmonary vascular remodeling.

Key Words:

Hypoxic pulmonary hypertension, MiR-203, FGF2, Cell proliferation, Cell migration.

Introduction

Pulmonary hypertension (PH) is a disorder of pulmonary hemodynamics induced by a variety of causes and can lead to a progressive increase in pulmonary vascular resistance and increased pressure in the pulmonary circulation, which make it a serious threat to human health. Increased long-term resistance to the pulmonary circulatory system may cause increased right ventricular loading and right ventricular hypertrophy, finally leading to right heart failure and death[1]. Increased pulmonary arterial pressure caused by hypoxia is an important part of the body's adaptation to the hypoxic environment at high altitude. The occurrence of severe hypoxic pulmonary hypertension (HPH) is the central link in the development of various types of diseases at high altitude. Hypoxic pulmonary vasoconstriction (HPV) occurs in the early stage of HPH, and hypoxic pulmonary vascular remodeling (HPVR) that occurs in the chronic phase is difficult to reverse[2, 3]. HPH is commonly seen in interstitial lung disease and chronic obstructive pulmonary disease (COPD). Severe HPH is commonly seen in mixed emphysema or pulmonary fibrosis syndrome, and the prevalence of PH in these patients is high[4-6]. Any lung disease progressed to PH will be accompanied by deteriorated exercise capacity, aggravated hypoxia increase and shortened survival time[7-9].

MiRNAs are a class of highly conserved non-coding RNAs (ncRNAs). The miRNA selectively binds to the RNA-induced silencing complex and combines with the 3'-untranslated region (3'-UTR) of target mRNA through the base complementary pairing, inhibiting the translation of the mRNA or degrading it and hence negatively regulating the target gene's expression[10, 11]. MiRNAs play an important role in the formation of HPH. In the lungs of HPH rats, the expression of miR-451 was upregulated and miR-22 was

Corresponding Author: Zhaozhong Cheng, MD; e-mail: chengzzqd@outlook.com

down-regulated[12]. MiR-145/-143 is a group of miRNAs that are highly expressed in smooth muscle cells and are known as vascular smooth muscle cell markers. In addition, they are important molecular switches that promote smooth muscle cell differentiation and stabilize the phenotype[13]. MiR-21 is upregulated in hypoxia-stimulated human PASMC and promotes cell proliferation and migration by inhibiting multiple target genes such as PDCD4[14]. In the blood of patients with HPH, miR-23b expression was significantly upregulated, while miR-1 was markedly downregulated[15].

MiR-203 is located at 14q32.33, and is expressed specifically in epithelial tissues. It participates in skin development, homeostasis, and function maintenance through induction and promotion of differentiation. It is an important regulatory factor in skin tissue. Meanwhile, it is recognized for its tumor suppressing and pro-apoptotic role in epithelial tissue diseases and inflammatory reactions[16]. Malignant tumors can inhibit the expression of miR-203 by activating ZEB1 factor, so as to inhibit tumor cell differentiation[17]. In metastatic prostate cancer, the re-expression of miR-203 can cause M-ET (mesenchymal to epithelial transition). In this process, the effect of miR-203 may be through the action of survivin/BIRC5, which is an apoptosis inhibitory factor[17]. There are also studies showing that miR-203 promotes the development of gastric lymphoma by inhibiting the action of tyrosine kinase ABL1 in cells of gastric B-cell lymphoma[18]. Previous studies showed that miR-203 was significantly down-regulated in HPH tissues[19], but the underlying mechanism remains to be studied.

Materials and methods

Construction of Rat HPH Model

16 male Sprague-Dawley (SD) rats weighing 180-220 g were randomly divided into hypoxic model group and normoxic control group according to body weight, with 8 rats in each group. The rats in the hypoxic model group were cultured in a hypoxic environment with an oxygen concentration of 10% (90% N_2 and 10% O_2 mixture) for 3 weeks. Anhydrous tin chloride and lime were respectively used to absorb water and CO_2 in the incubator. The rats in the normoxic control group were normally fed (21% O_2) for 3 weeks. During the experimental period, both groups of rats were free to drink and eat. This study was approved by the Animal Ethics Committee of The Affiliated Hospital of Qingdao University Animal Center.

Right Ventricular Systolic Pressure in Rats

The rats were anesthetized with 4% chloral hydrate and fixed in a supine position on the operating table. The right side of the neck was cut, and the right external jugular vein was exposed and dissociated. The vessel was cut at approximately 1/3 away from the distal end, and then a pre-filled copper heparin PE-50 catheter was quickly inserted into the vessel along the incision and was slowly advanced. The end of the PE-50 catheter was connected to the MedLab-U/501H biological signal acquisition and processing system. The position of the catheter tip was judged according to the change of the pressure waveform and pressure value displayed by the biological signal acquisition and processing system. The catheter was inserted approximately 2-3 cm into the right atrium, and 4-5 cm into the right ventricle, with the pressure close to 0 mmHg. The pulmonary artery systolic pressure was indirectly reflected by recording right ventricular systolic pressure (RVSP).

Calculation of Right Ventricular Hypertrophy Index (RVHI)

Rat hearts were washed repeatedly with Phosphate-Buffered Saline (PBS) to remove residual blood. Left and right atria and great blood vessels were cut along the atrioventricular sulcus. The right ventricular (RV) free wall was cut along the interventricular septum, and the left ventricle and ventricular septum (LV+S) were separated and opened to facilitate removal of residual liquid in the left ventricle. After weighing the heart, the data was recorded and the right ventricular hypertrophy index was calculated, RVHI = RV/(LV + S).

Hematoxylin and Eosin (HE) Staining

Tissue sections were placed into xylene and ethanol in turn. After washing with distilled water, the tissues were stained using hematoxylin for 15 min, and then rinsed with tap water for 3 s. 1% hydrochloric acid ethanol was then used to stain them for 3 s and rinsed again for 30 s. Blue promoting liquid was applied to make the tissue return to blue, after that, the tissues were in turn washed with tap water for 15 min, rinsed slightly with distilled water for 2 s, stained with 0.5% eosin for 3 min, and washed with 80% ethanol slightly for 2 s. The tissue slices were sequentially put into 95% ethanol for 5 min, anhydrous ethanol

for l0 min, xylene for 5 min. At last, the transparent slices were dropped on a gum and covered with a cover glass. After the gum was dried slightly, they were labeled.

Cell Culture

Chloralaldehyde anesthesia was performed to euthanize SD rats. Heart and lung tissues were quickly isolated under aseptic conditions and rinsed several times with PBS. The adventitia fibrous connective tissue was stripped and rinsed with PBS several times. The pulmonary artery was cut to remove the intima. Then the media was transferred to Dulbecco's Modified Eagle Medium (DMEM) (Gibco, Rockville, MD, USA) containing 10% fetal bovine serum (FBS) (Gibco, Rockville, MD, USA) and cut into small pieces repeatedly with ophthalmic scissors. The mesangial fragments were placed into pre-equipped enzyme solution in 37°C water bath for shaking at 90 r/min. When the segments of the artery were digested into flocs, the supernatant was removed by centrifugation, and DMEM complete medium was added and placed in a cell incubator at 37°C with 5% CO_2.

Transfection of cells

Cells in logarithmic phase were selected for transfection. We added 1.5 mL of serum-free medium and 500 μL of reagent containing miR-203 NC or mimics or inhibitor to cultured cells. The mixture of FGF2 interference plasmid and Lipofectamine TM 2000 (Invitrogen, Carlsbad, CA, USA) was added to cells, which were incubated in a 37°C incubator for 4 to 6 hours. After that, the supernatant was replaced with complete medium. After 24 to 48 hours of transfection, further operations were performed according to the purpose of the experiment. The sequences were as follows. MiR-203-mimics (5'-GUGAAAUGUUUAGGACCACUAG-3' 5'- AGUGGUCCUAAACAUUUCACUU-3'); miR-203-inhibitor (5'-CUAGUGGUCCUAAACAUUUCAC-3'); miR-203-mimics-NC (Sense (5'-UUCUCCGAACGUGUCACGUTT-3') antisense (5'-ACGUGACACGUUCGGAGAATT-3'); miR-203-inhibitor-NC (5'-CAGUACUUUUGUGUGUACAA-3'); FGF2-SiRNA (sense: 5'-AGCGGCTGTACTGCAAAAAC-3' antisense: 5,'-CCCAGGTCCTGTTTTGGAT-3').

Immunofluorescence

Cells with good growth status were seeded at $2*10^5$ cells per well in the 6-well plate with built-in coverslips. Cell identification was performed 24 hours later when they are naturally attached to the bottom. Subsequently, FITC labeled a-SMA monoclonal antibody was added to incubate the cells for 1 h at room temperature in the dark. After that, PBS was used to rinse them 3 times. Hoechst 33258 staining solution was added to stain the nucleus and incubated at room temperature for 5 min in the dark, and again PBS was used to rinse the cells for 3 times. The coverslips were removed from the 6-well plate, and a drop of glycerol was dropped on slides. Cells were then observed under a fluorescence microscope.

RNA Extraction

The tissue was ground and 1 mL of TRIzol (Invitrogen, Carlsbad, CA, USA) was added to each 50-100 mg tissue to lyse them. After adding 250 μL of chloroform in, the mixture was shaken for 30 seconds and centrifuged at 4°C. The aqueous phase was aspirated and an equal volume of pre-cooled isopropanol was added. After centrifugation the precipitate was washed gently with 75% ethanol, and dissolved in 20 μL of diethyl pyrocarbonate (DEPC) water. The RNA concentration was measured using a spectrophotometer. After that, RNA was placed in a refrigerator at -80°C until use.

Reverse Transcription and Quantitative Real Time-Polymerase Chain Reaction (qRT-PCR) Detection

The total RNA of the cells was extracted using the TRIzol kit. A reverse transcription reaction system was prepared on ice using the PrimeScript RT reagent Kit (TaKaRa, Code No. RR037A, Tokyo, Japan), and complementary Deoxyribose Nucleic Acid (cDNA) was obtained after the reaction completed. Then the cDNA template was diluted with RNase-free water to a final concentration of 3 ng/μL. Quantitative PCR procedures were performed according to the SYBR Green PCR Kit instructions, with 10 μL of the total reaction system. The qRT-PCR conditions were: pre-denaturation at 95°C for 15 min, denaturation at 94°C for 15 s, 55°C for 30 s, extension at 72°C for 30 s, with 40 cycles. The primer sequences are as follows: miR-203 (F: 5'-TCCGATGATCACCAGGAT-3', R: 5'-GTGCAGGGTCCGAGGT-3'); FGF2 (F: 5'-AGAAGAGCGACCCTCACATCA-3', R: 5'-CGGTTAGCACACACTCCTTTG-3'); U6 (F: 5'-TCCGATCGTGAAGCGTTC-3', R: 5'-GTGCAGGGTCCGAGGT-3'); GAPDH (F: 5'-GGAATCCACTGGCGTCTTCA-3', R: 5'-GGTTCACGCCCATCACAAAC-3').

Cell Counting Kit-8 (CCK-8) Assay

After transfection for 24 hours, the cells were digested, collected, and seeded into 96-well plates at $2*10^3$ per well. Each group was set up with 6 replicates. The cell viability was measured using the CCK-8 assay (Dojindo, Kumamoto, Japan) 48 h after plating. Afterwards, 10 μL of CCK-8 solution was added to each well 2 h before the assay and incubated at 37°C for 1 h. The absorbance of each well at a wavelength of 450 nm was measured with a microplate reader.

EDU (5-Ethynyl-2′-Deoxyuridine)

The well-grown PASMCs were seeded in a 24-well plate with 5×10^4 cells per well. When the degree of cell fusion reached 80%, the transfection was performed. The specific steps were the same as before. Subsequently, 200 μL of 50 μM eU medium was added to each well for 2 hours of culture, and then added. The staining reaction solution was used to incubate the cells for 30 minutes, and 200 μL of Hochst was used to stain the cell nuclei, which was then observed and photographed under a fluorescence microscope.

Scratch Test

The well-differentiated PASMCs were digested and centrifuged, and then resuspended in DMEM containing 10% FBS. The cells were transferred to a 6-well plate at $2*10^5$ cells per well. After incubation overnight and the degree of cell fusion reached approximately 80%, the culture medium was removed and a straight line was drawn on the surface of the cells with a 200 μL pipette tip. After 0 h and 24 h after transfection, the wound healing condition was observed and photographed under an inverted phase contrast microscope. Adobe Photoshop F7.0 software was used to measure the width of scratches.

Immunohistochemistry

10% of formaldehyde was used to fix the selected tissue, and dehydration was completed using the conventional gradient alcohol. After paraffin embedding, 4 μm of the tissue was sliced continuously according to the SP kit and DAB kit instructions. FGF2 was positive when brown-yellow particles existed in the cytoplasm. The photographs were taken randomly under the microscope at 200 times, and the average optical density was measured using an image analysis system.

Western Blot

The cell lysate containing the protease inhibitor phenylmethylsulfonyl fluoride (PMSF) was added, and the cells were collected and lysed on ice. Then the lysate was aspirated and centrifuged at 12 000 r/min for 20 min. The supernatant was taken and the total protein concentration was measured by the bicinchoninic acid (BCA) method (Pierce, Rockford, IL, USA). 50 μg of total protein was taken from each sample and loaded on sodium dodecyl sulphate-polyacrylamide gel electrophoresis (SDS-PAGE) gel for electrophoresis. After the electrophoresis ended, the protein sample was transferred to polyvinylidene difluoride (PVDF) membrane (Millipore, Billerica, MA, USA), which was then blocked with skim milk for 2 hours and eluted 6 times by Tris-buffered saline-tween 20 (TBST) for 10 minutes. Afterwards, specific primary antibodies were added dropwise and incubated overnight. The next day, the secondary antibody was added for incubation after the membrane was washed. Finally, exposure was performed.

Dual Luciferase Reporting Assay

The wild-type and mutant sequences of FGF2 3'UTR that contain the binding site of miR-203 was cloned into the Luciferase reporter vector, which were then co-transfected into the cells with the miR-203 mimic or control sequences, respectively. Subsequently, dual Luciferase reporter assay was performed to detect Luciferase activity to determine the role of miR-203 in the potential binding site of FGF2 3' UTR.

Statistical Analysis

Statistical Product and Service Solutions (SPSS) 19.0 statistical software was used for analysis (IBM, Armonk, NY, USA). Measurement data were analyzed by *t*-test. Data were expressed as mean ± standard deviation, and the difference was statistically significant at $p<0.05$.

Results

Successful Construction of HPH Rat Model and Identification of PASMCs

We determined RVSP and RVHI in HPH model rats and normoxic control rats, and found that RVSP in the former was significantly higher than that in the latter (Figure 1A). The same results were obtained with RVHI analysis (Figure 1B). The results of HE staining showed that compared with the normoxic control group, the pulmonary vascular smooth muscle layer in the hypoxic group was significantly thickened, the lumen was

narrowed, and with the surrounding inflammatory cells infiltrated (Figure 1C), suggesting that the rat model of HPH was successfully constructed. Immunofluorescence results showed that the purity of the rat PASMCs was high and could be used for subsequent experiments (Figure 1D).

MiR-203 was Downregulated and could Inhibit the Proliferation and Migration of PASMCs in Hypoxic PASMCs

We detected miR-203 expression in PASMCs of hypoxia-treated rats and normoxia-treated rats by qRT-PCR, and found that miR-203 was significantly low in PASMCs of the hypoxic group (Figure 2A, 2B). We then upregulated or decreased intracellular miR-203 expression by transfecting miR-203 mimics and inhibitors (Figure 2C, 2D). The results of the EDU experiments showed that the over-expression of miR-203 reduced the proliferation of PASMCs, and vice versa (Figure 2E). The same result was obtained from CCK8 assay (Figure 2F). Through the scratching test, we found that overexpressing miR-203 could weaken the migration of PASMCs, while inhibiting it enhanced their migratory ability (Figure 2G). Thus it was conceivable that miR-203 could inhibit the proliferation and migration of PASMCs.

MiR-203 Selectively Combined with FGF2 and Reduced its Expression

We used bioinformatics analysis to predict the possible binding sites for miR-203 and FGF2 (Figure 3A). FGF2 wild-type and mutant plasmids were constructed for dual Luciferase reporter assays, and the result indicated that miR-203 can target FGF2 and combine with its 3'UTR (Figure 3B). The PCR results showed that the level of FGF2 decreased after overexpression of miR-203

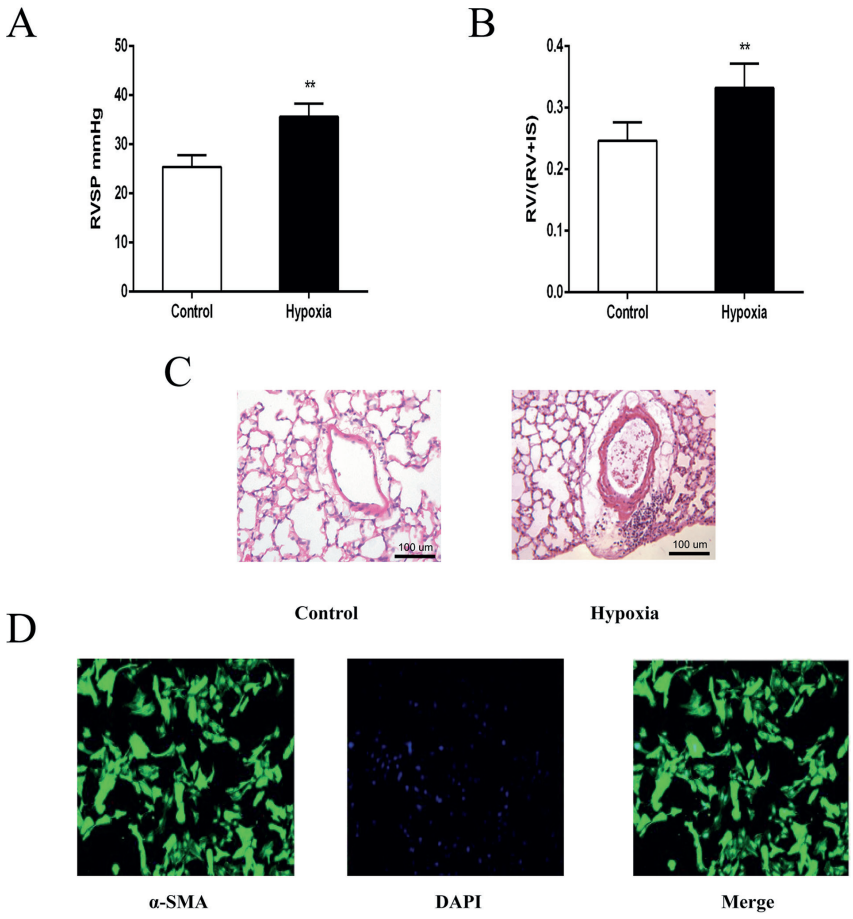

Figure 1. Establishment of rat model of HPH and identification of rat PASMCs. ***A,*** Statistical analysis of RVSP in normoxic control rats and HPH rats. ***B,*** Statistical analysis of RVHI in normoxic control rats and HPH rat models. ***C,*** HE staining of lung tissue of rats in HPH group and normoxic control group (observed under 20x microscopy). ***D,*** Identification of rat PASMCs by Immunofluorescence (observed by 20x microscopy).

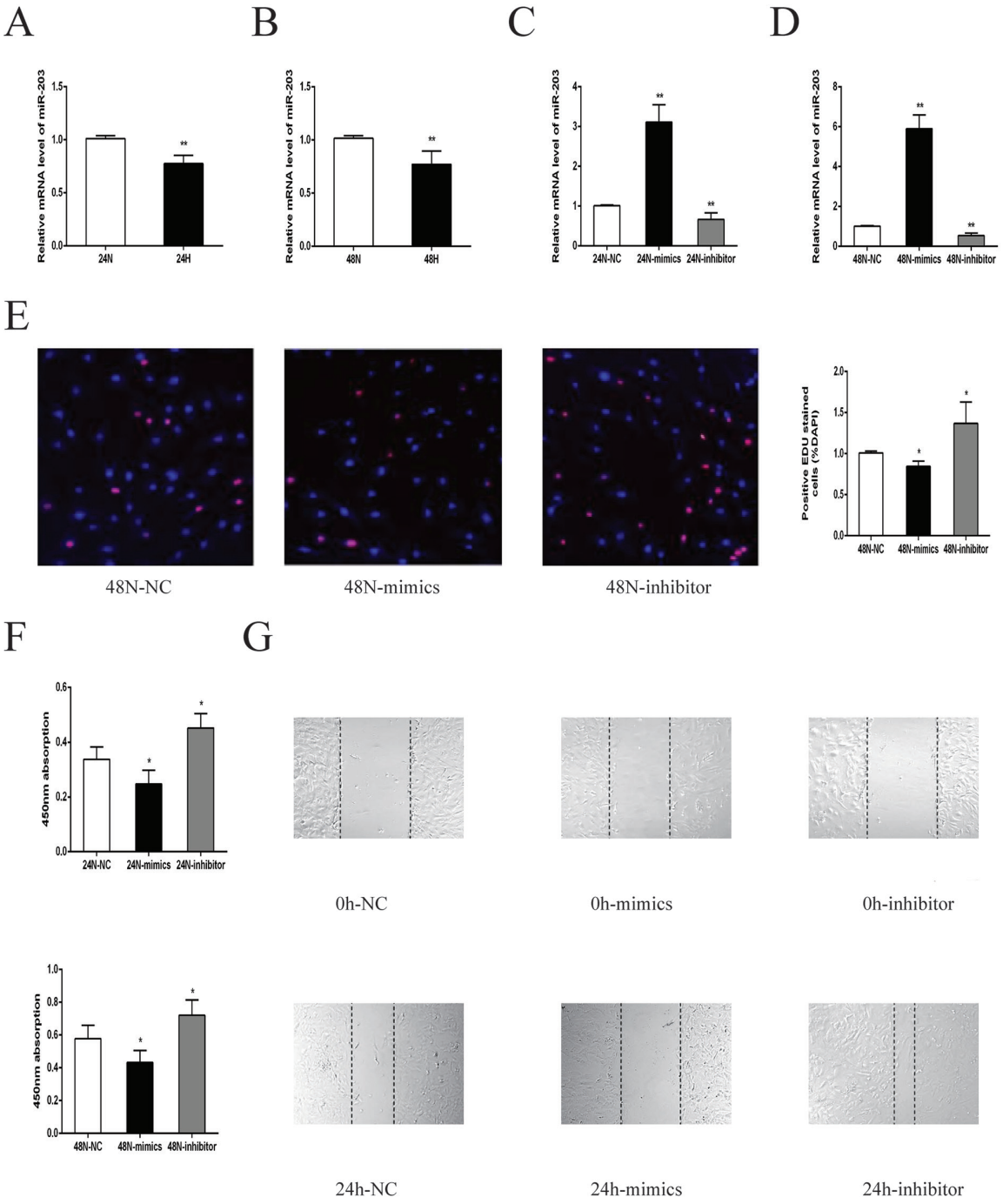

Figure 2. Expression of miR-203 in rat PASMCs treated with hypoxia and its effect on proliferation and migration of PASMCs. ***A,*** Relative expression of miR-203 in HPH rat PASMCs after 24h hypoxia compared with those in normoxic control group. ***B,*** Relative expression of miR-203 in HPH rat PASMCs after 48h hypoxia compared with those in normoxic control group. ***C,*** Relative expression of miR-203 in PASMCs after transfection with miR-203 mimics and miR-203 inhibitor for 24 h. ***D,*** Relative expression of miR-203 in PASMCs after transfection with miR-203mimics and miR-203 inhibitor for 48 h. ***E,*** The effect of overexpression and inhibition of miR-203 on the proliferation of rat primary PASMCs was detected by EDU assay (observed by 20x microscopy). ***F,*** The effect of overexpression and inhibition of miR-203 on rat primary PASMCs cell proliferation was detected by CCK8 assay. ***G,*** The effect of overexpression and inhibition of miR-203 on the migration of rat primary PASMCs was analyzed by scratch assay (20x microscopic observation).

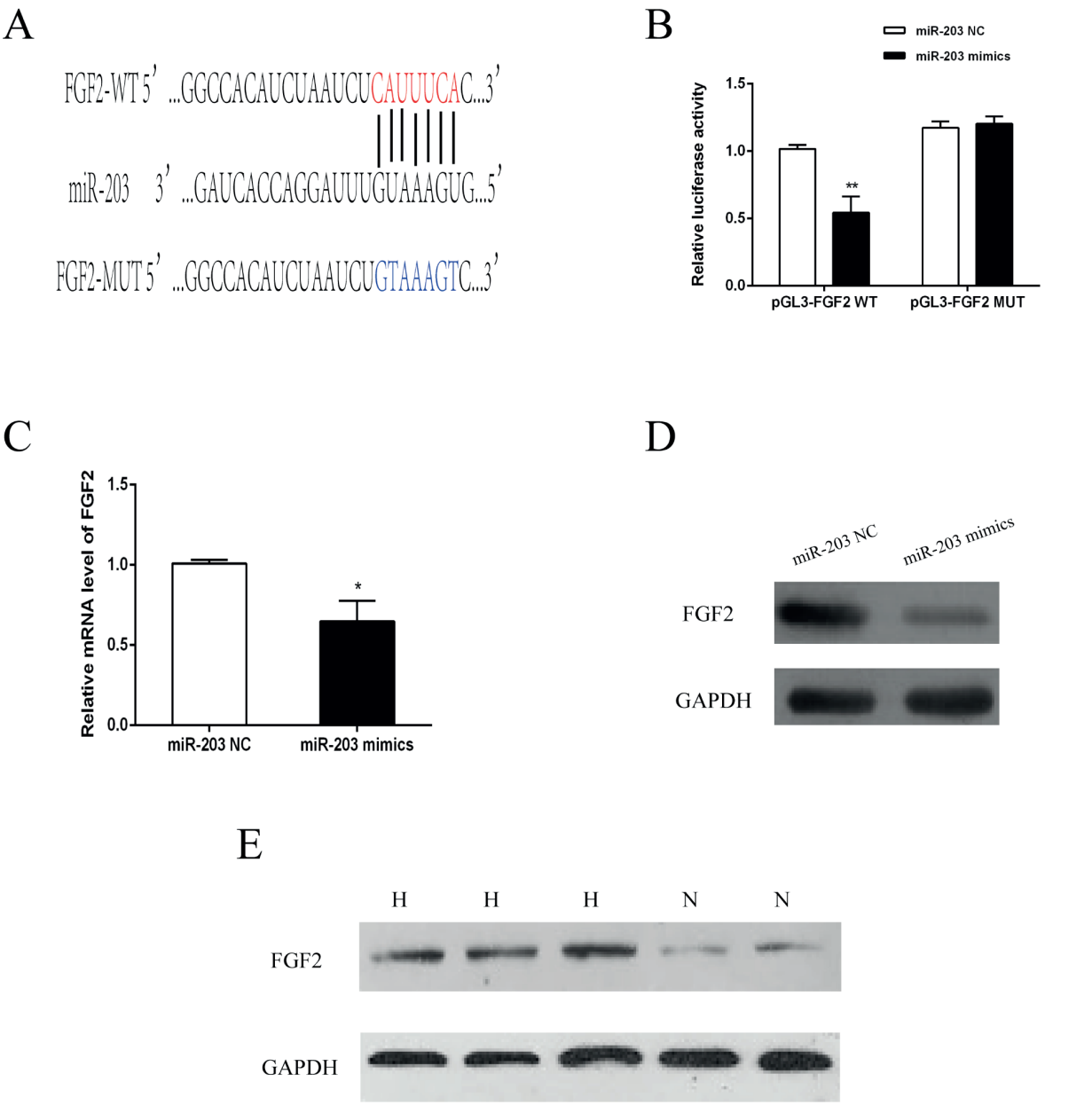

Figure 3. miR-203 could combine with FGF2 and degrade it. ***A,*** Bioinformatics prediction results of binding sites of miR-203 and FGF2 were shown. ***B,*** Dual Luciferase results showed that miR-203 could bind to the 3'UTR of FGF2. ***C,*** Overexpressing miR-203 significantly downregulated FGF2 expression. ***D,*** Overexpressing miR-203 significantly downregulated FGF2 protein expression. ***E,*** FGF2 protein expression in lung tissue of rats in HPH group and normoxic control group was shown.

(Figure 3C), and the same result at the protein level was found (Figure 3D). Meanwhile, Western blot assay indicated that the level of FGF2 protein in the HPH rat tissue was significantly higher than that in the normoxic group (Figure 3E). We thus concluded that miR-203 could selectively combine with and reduce its expression.

Inhibition of FGF2 Reduced Pulmonary Arterial Pressure and Improved Pulmonary Vascular Reconstruction

To further investigate the effect of FGF2 on HPH, we transfected FGF2-SiRNA in PASMCs. RT-PCR and Western blot assay revealed that both the mRNA and protein level of FGF2 in

the transfected cells was decreased (Figure 4A and 4B). In order to further reveal the effect of FGF2 on HPH rats, we tested the relevant indicators in the rats of the normoxic control group, the HPH control group, and the HPH+FGF2 siRNA group. It was found that compared with the con-

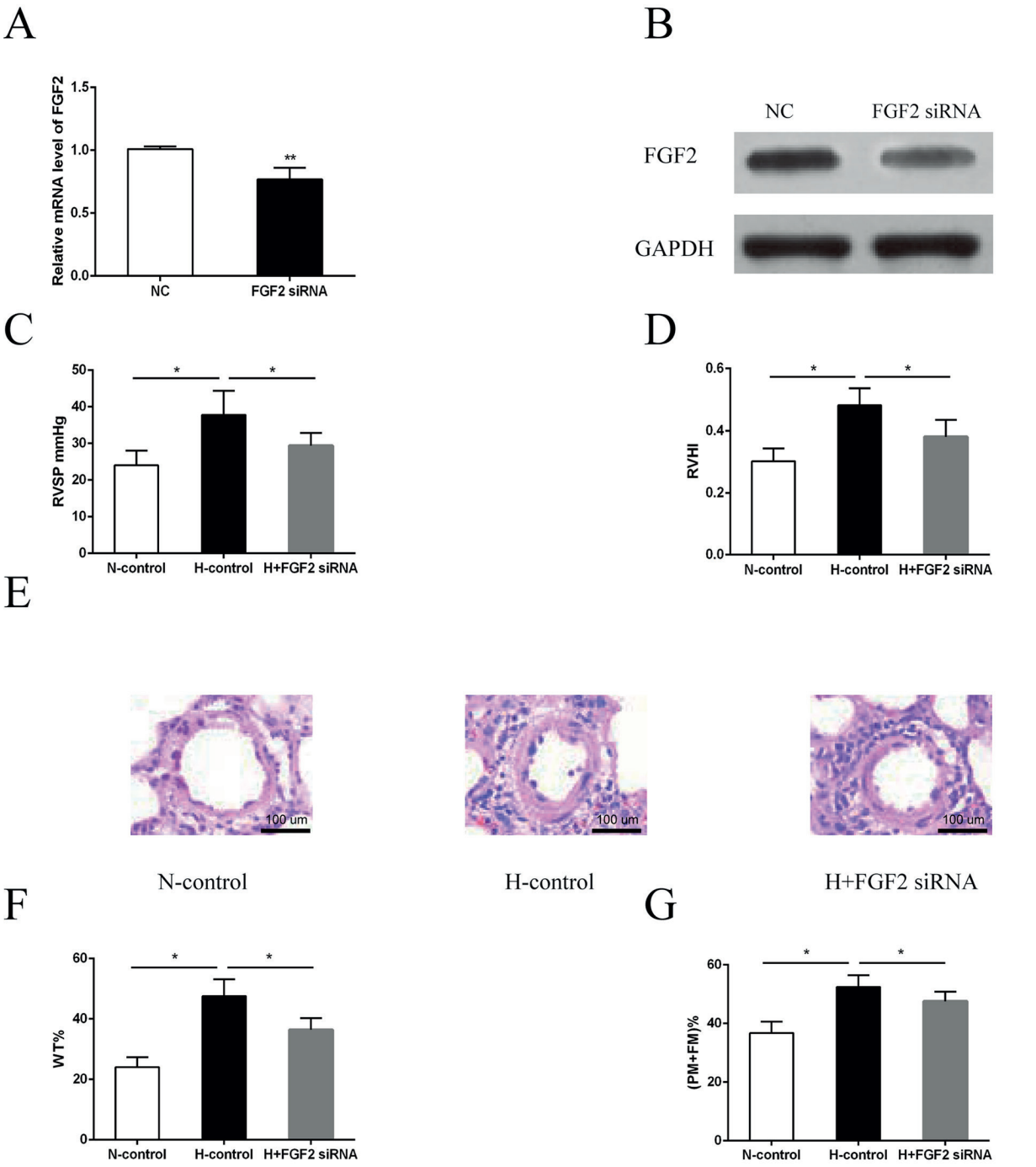

Figure 4. Effect of inhibition of FGF2 on HPH rat model was shown. ***A,*** FGF2 expression was significant downregulated after FGF2 inhibition. ***B,*** FGF2 protein expression was significantly down-regulated after FGF2 inhibition. ***C,*** Statistical analysis of RVSP in rats of three groups (N-control, H-control, H+FGF2 siRNA). ***D,*** Statistical analysis of RVHI in rats of three groups (N-control, H-control, H+FGF2 siRNA). ***E,*** Immunohistochemical results of lung tissue of rats in three groups (N-control, H-control, H+FGF2 siRNA) (observed by 20X microscopy). ***F,*** Statistical analysis of WT% in rats of three groups (N-control, H-control, H+FGF2 siRNA). ***G,*** Statistical analysis of (PM+FM)% in rats of three groups (N-control, H-control, H+FGF2 siRNA).

trol group, the indicators including RVSP, RVHI, WT%, (PM+FM)%, and thickness of pulmonary artery smooth muscle layer were all remarkably reduced in rats of HPH+FGF2 siRNA group (Figure 4C, 4D, 4E, 4F, 4G). From this we came to a conclusion that the inhibition of FGF2 reduced the pulmonary arterial pressure in HPH rats, which effectively improved pulmonary vascular remodeling.

Discussion

Hypoxic pulmonary hypertension (HPH) is a pathophysiological syndrome with extremely high difficulty to treat and high lethality and morbidity, which is a serious threat to human health. It is therefore called "pseudo-malignant" tumor[20]. The mechanism of HPH development has been a hot and difficult point in medical research[21]. Hypoxic pulmonary vascular structural reconstruction (HPVSR) is one of the basic pathophysiological features of HPH formation[22]. Hypoxia can lead to abnormal proliferation and apoptosis of pulmonary artery smooth muscle cells (PASMCs), and increased pulmonary vascular resistance and pulmonary artery pressure. The strategy of HPH treatment has shifted from expanding vascular smooth muscle to decrease pulmonary arterial pressure to inhibiting vascular dysplasia and pulmonary vascular structural reconstruction. The elucidation of the role and mechanism of abnormal proliferation and apoptosis of hypoxic PASMC in HPVSR is of great significance in seeking new strategies for effective prevention and treatment of HPH. Epigenetic regulation exists in almost all aspects of biological regulation[23]. Even if the intervention factor is removed, epigenetic modifications can remain stable for a long time and maintain the expression level of regulatory genes. Therefore, epigenetics shows its unique advantages and great potential in elucidating the mechanism of diseases.

FGF2, also known as basic fibroblast growth factor (FGF-2), is one of the fibroblast growth factor family members (FGFs) and was the earliest discovered angiogenic factor. Studies have shown that FGF2 can stimulate endothelial cell proliferation, migration, differentiation, and angiogenesis *in vitro* and *in vivo*[24]. FGFs are mitogenic agents of mesoderm and ectoderm-derived cells and play an important role in many physiological and pathological processes, such as promoting embryonic development, cell differentiation, neuronal growth, wound healing, tumor growth, cell survival, migration, infiltration, transformation and angiogenesis[25-27]. We wondered if FGF2 can still play such a role in HPH, so we further investigated FGF2 in this study.

In this study, it was found in HPH rats that RVSP and RVHI were increased, pulmonary mesangial smooth muscle was significantly thickened, and lumen was narrowed, with peripheral inflammatory cells infiltrated. RT-PCR result showed that miR-203 level in hypoxia-treated PASMCs was lower than that in the normoxic group. After overexpression of miR-203, the cell proliferation and migration of PASMCs were remarkably reduced. Further exploration of the mechanism demonstrated that miR-203 can selectively bind to FGF2 to inhibit its expression. At the same time, we found that FGF2 protein expression was significantly up-regulated in tissues of HPH rat model. After inhibiting FGF2 *in vivo*, we found that all the indicators in HPH rats decreased, including RVSP, RVHI, the thickness of pulmonary arterial smooth muscle, WT%, and (PM+FM)%. In addition, pulmonary artery pressure was found reduced in HPH rats, and pulmonary vascular remodeling has been significantly improved.

Conclusions

We showed that hypoxia is involved in the development of HPH by inhibiting the activation of FGF2 by miR-203. Additionally, specific inhibition of FGF2 can reduce hypoxia-induced pulmonary hypertension and improve pulmonary vascular remodeling.

Conflict of Interest

The Authors declare that they have no conflict of interest.

References

1) Humbert M, Sitbon O, Simonneau G. Treatment of pulmonary arterial hypertension. N Engl J Med 2004; 351: 1425-1436.

2) Ma L, Ambalavanan N, Liu H, Sun Y, Jhala N, Bradley WE, Dell'Italia LJ, Michalek S, Wu H, Steele

C, Benza RL, Chen Y. TLR4 regulates pulmonary vascular homeostasis and remodeling via redox signaling. Front Biosci (Landmark Ed) 2016; 21: 397-409.

3) Zungu-Edmondson M, Shults NV, Wong CM, Suzuki YJ. Modulators of right ventricular apoptosis and contractility in a rat model of pulmonary hypertension. Cardiovasc Res 2016; 110: 30-39.

4) Seeger W, Adir Y, Barbera JA, Champion H, Coghlan JG, Cottin V, De Marco T, Galie N, Ghio S, Gibbs S, Martinez FJ, Semigran MJ, Simonneau G, Wells AU, Vachiey JL. [Pulmonary hypertension in chronic lung diseases]. Turk Kardiyol Dern Ars 2014; 42 Suppl 1: 142-152.

5) Hurdman J, Condliffe R, Elliot CA, Swift A, Rajaram S, Davies C, Hill C, Hamilton N, Armstrong IJ, Billings C, Pollard L, Wild JM, Lawrie A, Lawson R, Sabroe I, Kiely DG. Pulmonary hypertension in COPD: results from the aspire registry. Eur Respir J 2013; 41: 1292-1301.

6) Zhuan B, Yu Y, Yang Z, Zhao X, Li P. Mechanisms of oxidative stress effects of the NADPH oxidase-ROS-NF-kB transduction pathway and VPO1 on patients with chronic obstructive pulmonary disease combined with pulmonary hypertension. Eur Rev Med Pharmacol Sci 2017; 21: 3459-3464.

7) Oswald-Mammosser M, Weitzenblum E, Quoix E, Moser G, Chaouat A, Charpentier C, Kessler R. Prognostic factors in COPD patients receiving long-term oxygen therapy. Importance of pulmonary artery pressure. Chest 1995; 107: 1193-1198.

8) Lettieri CJ, Nathan SD, Barnett SD, Ahmad S, Shorr AF. Prevalence and outcomes of pulmonary arterial hypertension in advanced idiopathic pulmonary fibrosis. Chest 2006; 129: 746-752.

9) Kessler R, Faller M, Weitzenblum E, Chaouat A, Aykut A, Ducolone A, Ehrhart M, Oswald-Mammosser M. "Natural history" of pulmonary hypertension in a series of 131 patients with chronic obstructive lung disease. Am J Respir Crit Care Med 2001; 164: 219-224.

10) Liu X, Park JK, Jiang F, Liu Y, McKearin D, Liu Q. Dicer-1, but not loquacious, is critical for assembly of miRNA-induced silencing complexes. RNA 2007; 13: 2324-2329.

11) Huntzinger E, Izaurralde E. Gene silencing by microRNAs: contributions of translational repression and mRNA decay. Nat Rev Genet 2011; 12: 99-110.

12) Caruso P, MacLean MR, Khanin R, McClure J, Soon E, Southgate M, MacDonald RA, Greig JA, Robertson KE, Masson R, Denby L, Dempsie Y, Long L, Morrell NW, Baker AH. Dynamic changes in lung microRNA profiles during the development of pulmonary hypertension due to chronic hypoxia and monocrotaline. Arterioscler Thromb Vasc Biol 2010; 30: 716-723.

13) Cordes KR, Sheehy NT, White MP, Berry EC, Morton SU, Muth AN, Lee TH, Miano JM, Ivey KN, Srivastava D. Mir-145 and mir-143 regulate smooth muscle cell fate and plasticity. Nature 2009; 460: 705-710.

14) Sarkar J, Gou D, Turaka P, Viktorova E, Ramchandran R, Raj JU. MicroRNA-21 plays a role in hypoxia-mediated pulmonary artery smooth muscle cell proliferation and migration. Am J Physiol Lung Cell Mol Physiol 2010; 299: L861-L871.

15) Wei C, Henderson H, Spradley C, Li L, Kim IK, Kumar S, Hong N, Arroliga AC, Gupta S. Circulating miRNAs as potential marker for pulmonary hypertension. PloS One 2013; 8: e64396.

16) Saini S, Majid S, Yamamura S, Tabatabai L, Suh SO, Shahryari V, Chen Y, Deng G, Tanaka Y, Dahiya R. Regulatory role of mir-203 in prostate cancer progression and metastasis. Clin Cancer Res 2011; 17: 5287-5298.

17) Wellner U, Schubert J, Burk UC, Schmalhofer O, Zhu F, Sonntag A, Waldvogel B, Vannier C, Darling D, Zur HA, Brunton VG, Morton J, Sansom O, Schuler J, Stemmler MP, Herzberger C, Hopt U, Keck T, Brabletz S, Brabletz T. The EMT-activator ZEB1 promotes tumorigenicity by repressing stemness-inhibiting microRNAs. Nat Cell Biol 2009; 11: 1487-1495.

18) Craig VJ, Cogliatti SB, Rehrauer H, Wundisch T, Muller A. Epigenetic silencing of microRNA-203 dysregulates ABL1 expression and drives helicobacter-associated gastric lymphomagenesis. Cancer Res 2011; 71: 3616-3624.

19) Legchenko E, Chouvarine P, Borchert P, Fernandez-Gonzalez A, Snay E, Meier M, Maegel L, Mitsialis SA, Rog-Zielinska EA, Kourembanas S, Jonigk D, Hansmann G. PPARγ agonist pioglitazone reverses pulmonary hypertension and prevents right heart failure via fatty acid oxidation. Sci Transl Med 2018; 10: eaao0303.

20) McLaughlin VV, Archer SL, Badesch DB, Barst RJ, Farber HW, Lindner JR, Mathier MA, McGoon MD, Park MH, Rosenson RS, Rubin LJ, Tapson VF, Varga J, Harrington RA, Anderson JL, Bates ER, Bridges CR, Eisenberg MJ, Ferrari VA, Grines CL, Hlatky MA, Jacobs AK, Kaul S, Lichtenberg RC, Lindner JR, Moliterno DJ, Mukherjee D, Pohost GM, Rosenson RS, Schofield RS, Shubrooks SJ, Stein JH, Tracy CM, Weitz HH, Wesley DJ; ACCF/AHA 2009 expert consensus document on pulmonary hypertension: a report of the American College of Cardiology Foundation Task Force on Expert Consensus Documents and the American Heart Association: developed in collaboration with the American College of Chest Physicians, American Thoracic Society, Inc., and the Pulmonary Hypertension Association. Circulation 2009; 119: 2250-2294.

21) Stenmark KR, Fagan KA, Frid MG. Hypoxia-induced pulmonary vascular remodeling: cellular and molecular mechanisms. Circ Res 2006; 99: 675-691.

22) Xia S, Tai X, Wang Y, An X, Qian G, Dong J, Wang X, Sha B, Wang D, Murthi P, Kalionis B, Wang X, Bai C. Involvement of Gax gene in hypoxia-induced pulmonary hypertension, proliferation, and apoptosis

of arterial smooth muscle cells. Am J Respir Cell Mol Biol 2011; 44: 66-73.

23) Zhao S, Xu W, Jiang W, Yu W, Lin Y, Zhang T, Yao J, Zhou L, Zeng Y, Li H, Li Y, Shi J, An W, Hancock SM, He F, Qin L, Chin J, Yang P, Chen X, Lei Q, Xiong Y, Guan KL. Regulation of cellular metabolism by protein lysine acetylation. Science 2010; 327: 1000-1004.

24) Brem H, Klagsbrun M. The role of fibroblast growth factors and related oncogenes in tumor growth. Cancer Treat Res 1992; 63: 211-231.

25) Turner N, Grose R. Fibroblast growth factor signalling: from development to cancer. Nat Rev Cancer 2010; 10: 116-129.

26) di Martino E, Tomlinson DC, Knowles MA. A decade of FGF receptor research in bladder cancer: past, present, and future challenges. Adv Urol 2012; 2012: 429213.

27) Goetz R, Mohammadi M. Exploring mechanisms of FGF signalling through the lens of structural biology. Nat Rev Mol Cell Biol 2013; 14: 166-180.